

Discrete-Time Repetitive Control With Model-Less FIR Filter Inversion for High Performance Nanopositioning

Yik R. Teo¹, Arnfinn A. Eielsen², J. Tommy Gravdahl², Andrew J. Fleming¹

Abstract—Repetitive control (RC) is used to track and reject periodic exogenous signals. RC achieves tracking by incorporating a model of a periodic signal in the feedback path, which provides infinite loop-gain at the harmonic frequencies of the periodic signal. To improve robustness, the periodic signal model is bandwidth limited, and to improve the performance, an inverse plant response filter is used. This filter can either be an infinite impulse response (IIR) filter or a finite impulse response (FIR) filter. The accuracy of the filter typically determines the allowable bandwidth of the periodic signal model, and it is therefore desirable to obtain the most accurate inverse possible. In this paper a model-less method for synthesizing an FIR filter for the inverse response is presented, and it is compared to the common approach of using an inverse model-based IIR filter. An experimental comparison of the two approaches is presented, and it is demonstrated that the two methods produce identical results, but where the model-less FIR filter approach has the added benefit of avoiding the modeling effort needed to obtain the IIR filter.

I. INTRODUCTION

Repetitive control (RC) [1] is a well-known technique used to track and reject periodic exogenous signals. This is achieved due to the internal model principle (IMP) [2], which states that an exogenous signal can be nulled in the error signal if a model of the dynamic structure of the reference and disturbance signals is in the feedback path. RC was originally developed to reject the periodic disturbances in a power supply control application [3], but has since been used for machining of parts [4], precision positioning [5], optical drives [6], [7], electro-hydraulics [8], and scanning probe microscopy [9], [10], [11].

Fig. 1 shows the ideal signal model used in the RC scheme for a periodic signal with period L . This is a computationally efficient implementation, as the model only consists of a positive feedback around a time-delay. This results in an infinite number of marginally-stable poles with infinite gain at the harmonics of the periodic reference.

The most common approach to implementing discrete-time RC was first proposed in [12], where the plant dynamics is inverted using the zero-phase tracking error control (ZPETC) method. This approach can in principle obtain a bandwidth up to the Nyquist frequency. However, the approach lacks robustness, especially to plant modeling errors. In order to address this problem, the gain of the RC law can be

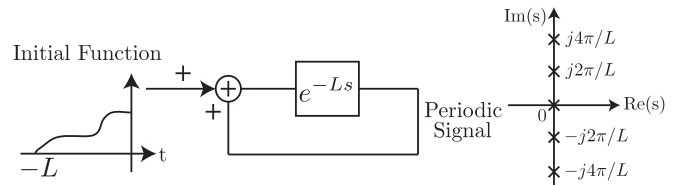


Fig. 1. A time-delay with positive feedback with the appropriate initial function can model any periodic signal [1].

bandwidth limited using a low-pass filter [1], [13], [14]. This will improve the stability margin at higher frequencies, where the plant model typically has the largest uncertainty. The application of general uncertainty and performance weights can also be accommodated for using the H_∞ synthesis framework [15], [16]. The robustness of the closed-loop system can also be improved by computing a frequency weighted inverse of the plant [17]. An analog implementation of RC is also possible [18], [19].

The ZPETC method requires an accurately identified infinite impulse response (IIR) model of the plant. This can be a disadvantage in some cases, as the accuracy of the identified model depends on the choice of model structure, the quality of the excitation signal, and the method of identification. In addition, since non-minimum phase zeros can not be inverted, the magnitude response of the ZPETC inverse can be inaccurate. The inversion effectiveness therefore depends on the model accuracy and the effect of the non-minimum phase zeros. As an alternative to the IIR model inverse, a finite impulse response (FIR) filter inverse model can be used [20], [21]. An FIR filter can alleviate problems due to non-minimum phase zeros and the selection of model structure. The main disadvantage is that an FIR filter is usually more computationally demanding than an IIR filter.

In either case, for both the IIR and the FIR filter, one of the most reliable methods of identification is to first produce an empirical transfer-function estimate (ETFTE) [22]. In [20], [21] it is suggested to synthesize the inverse plant response FIR filter by minimizing a least-squares cost function using an ETFTE generated using Gaussian white noise excitation via the Welch averaged periodogram method [23], i.e., the ETFTE is found by the quotient of the cross power spectral density estimate of the input and the measured output, and the power spectral density estimate of the input.

In this paper, alternative methods for producing both the ETFTE and the inverse plant response FIR filter are presented. Here, the ETFTE is computed with very high accuracy by using pseudo-random binary signal (PRBS) excitation and subsequent periodic averaging in the time-domain. The in-

¹Y. R. Teo and A. J. Fleming are with the Precision Mechatronics Labs, Faculty of Engineering and Built Environment, The University of Newcastle, Callaghan 2308, New South Wales, Australia. { yik.teo, andrew.fleming }@newcastle.edu.au

²A. A. Eielsen and J. T. Gravdahl are with the Department of Engineering Cybernetics, Norwegian University of Science and Technology Trondheim, Norway. { eielsen, gravdahl }@itk.ntnu.no

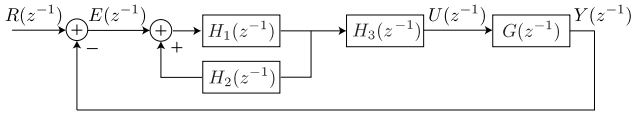


Fig. 2. Block diagram of RC system.

verse plant response FIR filter is then computed directly using the inverse discrete Fourier transform (IDFT) of the inverse of the ETFE, and a suitable windowing function to reduce artifacts due to the implicit rectangular windowing in the IDFT, which is equivalent to the frequency-sampling method for FIR filter design [24]. The result is a very high accuracy inverse response which can produce the same results as the ZPETC inverse, but without the modeling effort. The presented methods for generating the FIR filter and the EFTE are simpler and less computationally demanding compared to the approach in [20], [21], and produce the same, or better, accuracy for the EFTE and the subsequent FIR filter.

II. DISCRETE-TIME REPETITIVE CONTROL DESIGN

Fig. 2 shows a block diagram including the RC scheme and the plant $G(z^{-1})$. The filters $H_1(z^{-1})$ and $H_2(z^{-1})$ are used to produce a bandwidth-limited signal generator. If $H_1(z^{-1})$ and $H_2(z^{-1})$ have linear phase, and thus constant group delay, then a group delay of L will produce poles at $\pm j2\pi n/L$, $n \in \mathbb{R}^+$. Symmetric FIR filters have a linear phase response, thus $H_1(z^{-1})$ and $H_2(z^{-1})$ are ideally such filters. The magnitude response of $H_1(z^{-1})$ and $H_2(z^{-1})$ can then be used to limit the bandwidth. $H_3(z^{-1})$ is the inverse plant response filter, implemented as either an FIR or IIR filter.

From Fig. 2 it can be seen that the RC law can be written

$$C_{RC}(z^{-1}) = \frac{H_1(z^{-1})H_3(z^{-1})}{1 - H_1(z^{-1})H_2(z^{-1})}. \quad (1)$$

Assuming that the reference signal period will always be an integer multiple of the sampling time T_s , then the product of $H_1(z^{-1})H_2(z^{-1})$ in the denominator has to contain a delay of z^{-N} , where $N = L/T_s$, to satisfy the internal model principle.

The sensitivity function of the closed-loop system is

$$\begin{aligned} S(z^{-1}) &= \frac{E(z^{-1})}{R(z^{-1})} \\ &= \frac{1 - H_1(z^{-1})H_2(z^{-1})}{1 - H_1(z^{-1})H_2(z^{-1}) - H_1(z^{-1})H_3(z^{-1})G(z^{-1})} \\ &= \frac{1 - H_1(z^{-1})H_2(z^{-1})}{1 - H_1(z^{-1})(H_2(z^{-1}) - H_3(z^{-1})G(z^{-1}))}, \end{aligned}$$

which can be rearranged to be on the form shown in Fig. 3. It can then be seen that the stability of the RC system is determined by the denominator

$$1 - H_1(z^{-1})(H_2(z^{-1}) - H_3(z^{-1})G(z^{-1})),$$

which will provide stability if the loop transfer function in Fig. 3 satisfies the small-gain theorem [12], [17]. Thus, the system is stable if

$$\|H_1(z^{-1})(H_2(z^{-1}) - H_3(z^{-1})G(z^{-1}))\|_\infty < 1. \quad (2)$$

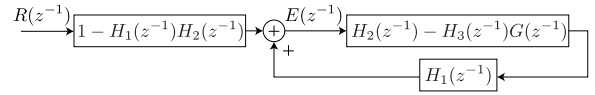


Fig. 3. Equivalent description of sensitivity function.

The stability condition can be split into two conditions, i.e.,

$$\|H_1(z^{-1})\|_\infty < 1, \quad (3)$$

and

$$\|H_2(z^{-1}) - H_3(z^{-1})G(z^{-1})\|_\infty < 1. \quad (4)$$

These two stability conditions are necessary for the design of the RC law as done in this paper.

III. IIR AND FIR INVERSE PLANT RESPONSE FILTERS

In this Section, we show two methods for designing the inverse plant response filter. The first is using the model-based zero-phase error tracking controller (ZPETC) IIR filter, and the second is using an model-less FIR filter synthesized directly from the plant frequency response.

A. Model-Based IIR Filter

An IIR model of the plant is given as

$$\widehat{G}(z^{-1}) = z^{-d} \frac{B(z^{-1})}{A(z^{-1})}, \quad (5)$$

where z^{-d} is the dead-time of the plant, and

$$\begin{aligned} B(z^{-1}) &= b_0 + b_1 z^{-1} + \dots + b_m z^{-m}, \quad b_0 \neq 0 \\ A(z^{-1}) &= 1 + a_1 z^{-1} + \dots + a_n z^{-n}. \end{aligned}$$

The perfect feed-forward tracking control for (5) is

$$\widehat{G}^{-1}(z^{-1}) = z^d \frac{A(z^{-1})}{B(z^{-1})}$$

which is non-causal due to the inverse of the d -step delay. The inverse cancels all the poles and zeros such that the product of the inverse filter and the plant is unity, i.e., there is zero-phase shift. This is only possible if the roots of $B(z^{-1}) = 0$ are inside the unit circle in the z -plane, i.e., if they are minimum phase zeros.

The method of inversion that excludes the non-minimum phase zeros is called the zero-phase error tracking controller (ZPETC) [25]. Applying this inverse, the product of the inverse filter and the plant will have zero-phase shift. This is done by factorizing the zeros of $\widehat{G}(z^{-1})$ as

$$B(z^{-1}) = B_a(z^{-1})B_u(z^{-1})$$

where $B_a(z^{-1})$ includes minimum phase, or acceptable, zeros, and $B_u(z^{-1})$ includes non-minimum phase, or unacceptable, zeros. The ZPETC inverse is then found in [25] to be

$$C_{ZPETC}(z^{-1}) = z^{(d+s)} \frac{A(z^{-1})\bar{B}_u(z^{-1})}{B_a(z^{-1})[B_u(1)]^2}$$

where $B_u(1)$ is the DC-gain of $B_u(z^{-1})$, and

$$\bar{B}_u(z^{-1}) = \bar{b}_s + \bar{b}_{(s-1)} z^{-1} + \dots + \bar{b}_0 z^{-s}.$$

The filter is non-causal and $(d + s)$ steps ahead. This can be overcome by delaying the input. As a result, the filter $H_3(z^{-1})$ is taken to be

$$H_3(z^{-1}) = z^{-(d+s)} C_{ZPETC}(z^{-1}).$$

RC requires that the product of the filters $H_1(z^{-1})$ and $H_2(z^{-1})$ has a delay of N steps. The stability criterion (4) is most easily satisfied if

$$H_2(z^{-1}) = z^{-(d+s)},$$

since $|H_2(z^{-1})| = |e^{-j\omega(d+s)}| = 1$, and thus (4) is

$$\|z^{-(d+s)} - z^{-(d+s)} C_{ZPETC}(z^{-1}) G(z^{-1})\|_{\infty} = \|1 - C_{ZPETC}(z^{-1}) G(z^{-1})\|_{\infty} < 1,$$

where $C_{ZPETC}(z^{-1}) G(z^{-1}) \approx 1$ if the ZPETC inverse is accurate. Assuming $N > d + s$, then $H_1(z^{-1})$ can be chosen to be a linear-phase FIR filter with a delay of $N - d - s$, i.e., it will have an order of $2(N - d - s)$, which means that it will have $2(N - d - s) + 1$ taps. $H_1(z^{-1})$ is a low-pass filter used to satisfy (2) at higher frequencies, where the uncertainty of the ZPETC inverse typically is high.

B. Model-Less FIR Filter

The alternative to the model-based IIR filter is to use an FIR filter. This can be considered a model-less approach, because no model structure needs to be chosen. This is also known as nonparametric frequency-domain system identification. As the FIR filter approximates the impulse response of a system directly, the accuracy of the filter is mainly determined by the length, or number of taps. The main benefits of using an FIR filter for plant inversion is the avoidance of inversion of non-minimum phase zeros and simple synthesis if a reliable plant frequency response can be obtained.

In terms of frequency samples, the empirical transfer-function estimate (ETF) [22] of the plant is given as

$$\hat{G}(k) = \frac{Y(k)}{U(k)},$$

and its inverse is given as

$$\hat{G}^{-1}(k) = \frac{U(k)}{Y(k)},$$

where $Y(k)$ and $U(k)$ are the discrete Fourier transforms (DFT) of, respectively, the output and input, i.e.,

$$Y(k) = \sum_{n=0}^{M-1} y(n) e^{-j2\pi kn/M},$$

and

$$U(k) = \sum_{n=0}^{M-1} u(n) e^{-j2\pi kn/M},$$

for $k = 0, 1, \dots, M - 1$. The estimates are empirical, as no other assumptions have been imposed besides linearity.

To obtain an accurate ETF, a periodic input signal and averaging can be used [22]. Here, the system is excited

by a pseudo-random binary signal (PRBS). A PRBS is deterministic, and it is spectrally white. Moreover, a PRBS has an optimal crest factor which results in a large total energy delivery into the excited system. If the system is excited by a periodic repetition of the PRBS with length N for P periods, the total length of the output signal is NP . By averaging over the periods, the output signal has length N , but the signal-to-noise ratio is increased by a factor P .

The inverse plant response filter $H_3(z)$ as an FIR filter can be found by taking the inverse discrete Fourier transform (IDFT) of $\hat{G}^{-1}(k)$. This method is also known as the frequency-sampling method for FIR filter design [24]. The unit impulse response $g_i(n)$ of $\hat{G}^{-1}(k)$ is

$$g_i(n) = \frac{1}{M} \sum_{k=0}^{M-1} \hat{G}^{-1}(k) e^{j2\pi kn/M},$$

where $n = 0, 1, \dots, M - 1$. The FIR filter is then expressed in the z -domain as

$$G_i(z^{-1}) = \sum_{n=0}^{M-1} g_i(n) z^{-n}.$$

The frequency-sampling method results in an unit impulse response which has been convoluted with a rectangular window of the same length in the frequency domain. The frequency response of $G_i(z^{-1})$ is therefore affected by the large side-lobes of the rectangular window. As a result, the modeling error of $G_i(z^{-1})$ is large between the frequency samples. This can be alleviated by the use of a window that do not contain abrupt discontinuities in the time domain, and thus have small side-lobes in the frequency domain, i.e., the window smoothes the frequency response of $G_i(z^{-1})$.

A windowed FIR filter $\tilde{h}(n)$ is created from an unwindowed FIR filter $h(n)$ as

$$\tilde{h}(n) = w(n) h(n)$$

where $w(n)$ is a window function which is nonzero only for $n = 0, 1, \dots, M - 1$. The frequency-domain representation of the window function $W(k)$ is found as

$$\begin{aligned} W(k) &= \sum_{n=0}^{M-1} w(n - M/2) e^{-j2\pi kn/M} \\ &= \left[\sum_{n=0}^{M-1} w(n) e^{-j2\pi kn/M} \right] e^{-j(2\pi k/M)(M/2)}, \end{aligned}$$

where the term $e^{-j(2\pi k/M)(M/2)}$ comes from the fact that the rectangular window is not centered around $n = 0$, but is time-shifted to be centered around $n = M/2$. This phase term will cause distortion of $h(n)$, unless $h(n)$ is also phase-shifted to compensate. The unit impulse response $g_i(n)$ is therefore phase-shifted before windowing. Due to the circular shift property of the DFT, this can be done by rearranging $g_i(n)$ such that

$$\bar{g}_i(n) = \begin{cases} g_i(n + M/2), & n = 0, 1, \dots, \frac{M}{2} - 1 \\ g_i(n - M/2), & n = \frac{M}{2}, \frac{M}{2} + 1, \dots, M - 1 \end{cases}$$



Fig. 4. Two-axis serial-kinematic nanopositioning platform.

for the case when M is even. The inverse response is then represented by the FIR filter

$$\bar{G}_i(z^{-1}) = \sum_{n=0}^{M-1} \bar{g}_i(n)z^{-n} = z^{-M/2}G_i(z^{-1})$$

which is $G_i(z^{-1})$ delayed by $M/2$ steps. Applying the window $w(n)$ to the time-shifted impulse response $\bar{g}_i(n)$,

$$\tilde{g}_i(n) = w(n)\bar{g}_i(n),$$

the filter

$$\tilde{G}_i(z^{-1}) = W(z^{-1}) * [z^{-M/2}G_i(z^{-1})]$$

is obtained, and $H_3(z^{-1}) = \tilde{G}_i(z^{-1})$ is used in (1).

For the implementation, $M = N$, and the stability condition given in (4) is simplified by choosing

$$H_2(z^{-1}) = z^{-N/2}, \quad (6)$$

since $|H_2(z^{-1})| = 1$, which results in

$$\begin{aligned} \|z^{-M/2} - G(z^{-1})z^{-M/2} [G_i(z^{-1}) * W(z^{-1})]\|_{\infty} = \\ \|1 - G(z^{-1}) [W(z^{-1}) * G_i(z^{-1})]\|_{\infty} < 1, \end{aligned}$$

where $G(z^{-1}) [W(z^{-1}) * G_i(z^{-1})] \approx 1$ if the FIR filter inverse is accurate. RC requires that the product of the filters $H_1(z^{-1})$ and $H_2(z^{-1})$ has a delay of N steps. Hence, $H_1(z^{-1})$ is chosen to be a linear-phase FIR filter with a delay of $N/2$ steps, i.e., it will have $N + 1$ taps. $H_1(z^{-1})$ is a low-pass filter used to satisfy (2) at higher frequencies, where the uncertainty of the FIR filter inverse typically is high, just as in the case of the ZPETC inverse.

IV. EXPERIMENTAL RESULTS

A. Nanopositioner Model

The experiments was conducted on the two-axis serial-kinematic nanopositioning stage shown in Fig. 4. The nanopositioner was designed and constructed at the EasyLab, University of Nevada, Reno, USA. Each axis contains a 12 mm long piezoelectric stack actuator (Noliac NAC2003-H12) with a free displacement of $12 \mu\text{m}$ at 200 V. The flexure design includes a mechanical amplifier to provide a total range of $30 \mu\text{m}$. The flexures also mitigate cross-coupling so

that each axis can be controlled independently. The position of the moving platform is measured by a Microsense 6810 capacitive sensor and 6504-01 probe, which has a sensitivity of $2.5 \mu\text{m/V}$. The stage is driven a by PiezoDrive PDL200 voltage amplifier with a gain of 20. The control law was implemented on a dSPACE DS1104 hardware-in-the-loop system via Simulink Coder. The anti-aliasing and reconstruction filters were implemented using two Stanford Research System SR570 pre-amplifiers. The experiments were done using the x -axis. The sampling frequency of the system was 10 kHz and the reference was a 40 Hz triangle wave, i.e., $T_s = 0.0001$ s and $L = 0.025$ s which resulted in $N = 250$.

The frequency response of the open-loop system was obtained using the method outline in Sec. III-B. Fig. 5 displays the measured response. For the purpose of control design, a continuous time model was found using a subspace identification method [26]. A model of order 6 gave the best fit in the frequency domain from 0 to 2 kHz. The model was then discretized using zero-order hold interpolation. The discrete-time model of the system was found as:

$$\hat{G}(z^{-1}) = \frac{A(z^{-1})}{B(z^{-1})} = \frac{-0.02 + 0.08z^{-1} - 0.16z^{-2} + 0.21z^{-3} - 0.17z^{-4} + 0.15z^{-4} - 0.10z^{-6}}{1 - 2.8z^{-1} + 3.4z^{-2} - 3.3z^{-3} + 3.2z^{-4} - 1.9z^{-5} + 0.43z^{-6}}$$

The frequency response of the model is also shown in Fig. 5.

B. Control Design

1) *Discrete-time RC with ZPETC inverse*: Fig. 6 shows the frequency response of the ZPETC inverse, as described in Sec. III-A. It can be seen that the product of the measured response and the ZPETC inverse is unity up to approximately 1 kHz, which is set as the cut-off frequency for the $H_1(z^{-1})$ low-pass filter to attenuate the unmodeled high-frequency dynamics. The dead-time of the system model is $d = 0$, and the numerator has $s = 3$ non-minimum phase zeros. The filters $H_3(z)$ and $H_2(z)$ are thus $H_3(z^{-1}) = z^{-3}C_{ZPETC}(z^{-1})$ and $H_2(z^{-1}) = z^{-3}$. As a result, the filter $H_1(z^{-1})$ has to have a delay of $N - (s + d) = 247$. The filter $H_1(z^{-1})$ is designed to be a linear-phase low-pass filter with a cut-off

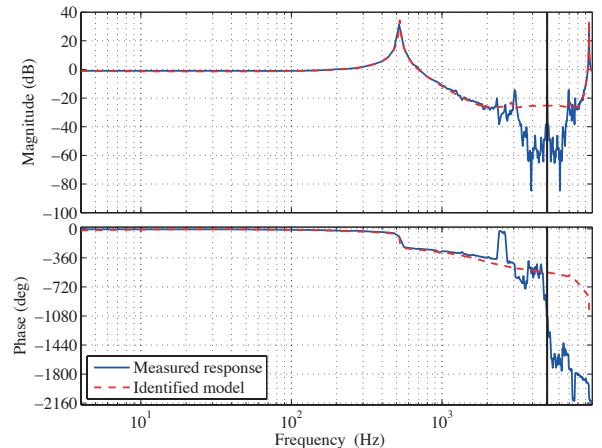


Fig. 5. The frequency response of the nanopositioner along the x -axis.

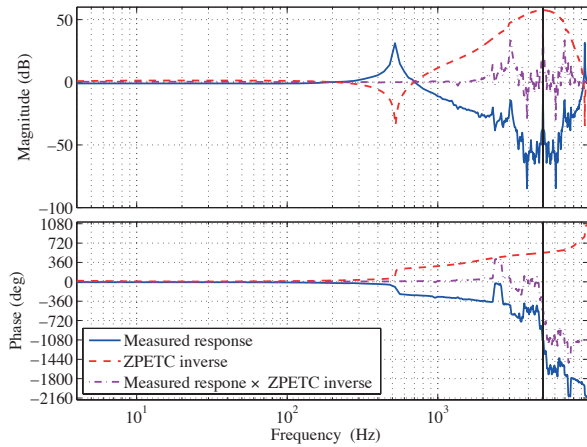


Fig. 6. Frequency responses when using the ZPETC inverse.

frequency of 1 kHz. The length of the filter is $2(N - d - s) + 1 = 495$ which results in the desired delay. Fig. 9 shows the response of $H_1(z^{-1})$ and the stability criterion (4).

2) *Discrete-time RC with FIR inverse*: Fig. 8 shows the frequency response of the FIR inverse filter $H_3(z^{-1})$ found using the method described in Sec. III-B. For $H_3(z^{-1})$ with a rectangular window, the modeling error is zero at the frequency samples, i.e., at 40 Hz, 80 Hz, 120 Hz, etc., but the error is large between the samples. This is due to the large side-lobes of the rectangular window. As can be seen, when applying a window, in this case a Hanning window, to the FIR filter, the frequency response is smoothed between the frequency samples. The product between the measured response and $H_3(z^{-1})$ with a Hanning window is shown to be approximately unity up to about 1 kHz, similar to the case of the ZPETC inverse. The filter $H_2(z^{-1})$ has a delay of 125 steps, and the filter $H_1(z^{-1})$ is designed to be a linear-phase low-pass filter with delay of $N/2$ steps and a cut-off frequency of 1 kHz. The length of the filter is $N + 1 = 251$. Fig. 10 shows the response of $H_1(z^{-1})$ and the stability criterion (4).

C. Results and Discussion

The reference signal is a $\pm 5 \mu\text{m}$ triangular wave at 40 Hz. The tracking performance of both controllers are shown in Fig. 11 and the error plots are shown in Fig. 12. The

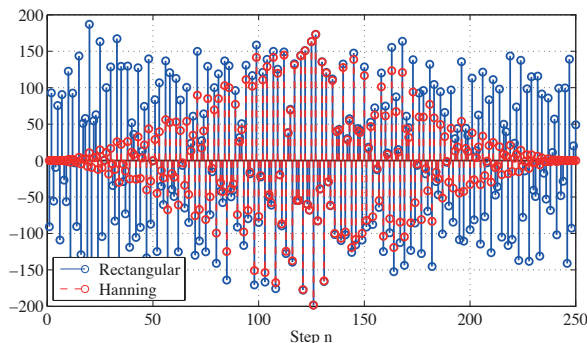


Fig. 7. The unit impulse response $h_3(n)$ when using a rectangular window and a Hanning window.

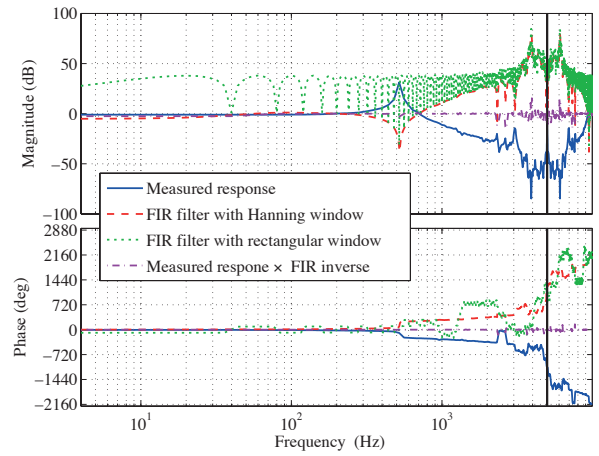


Fig. 8. Frequency responses when using the FIR inverse.

TABLE I
TRACKING RESULTS FOR $\pm 5 \mu\text{m}$ TRIANGLE WAVE REFERENCE AT 40 Hz.

Control law	$e_{max}(\%)$	$e_{rms}(\%)$
RC with FIR inverse	0.8571	0.1031
RC with ZPETC inverse	0.8341	0.1030

maximum tracking error is defined as

$$e_{max}(\%) = \frac{\max|y - r|}{\max(y) - \min(y)} \times 100\%$$

where y and r are the measured output and the reference, respectively. The root-mean-squared error (RSME) is defined as

$$e_{rms}(\%) = \frac{\sqrt{\frac{1}{T} \int_0^T [y(t) - r(t)]^2 dt}}{\max(y) - \min(y)} \times 100\% .$$

The tracking performance is summarized in Tab. I.

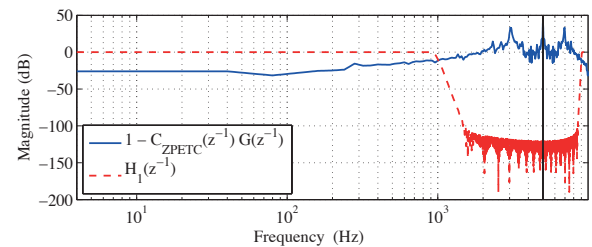


Fig. 9. $H_1(z^{-1})$ and the stability criterion (4) with ZPETC inverse.

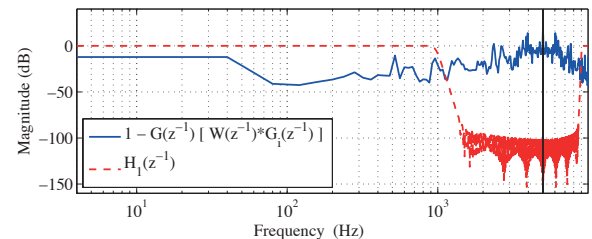


Fig. 10. $H_1(z^{-1})$ and the stability criterion (4) with FIR inverse.

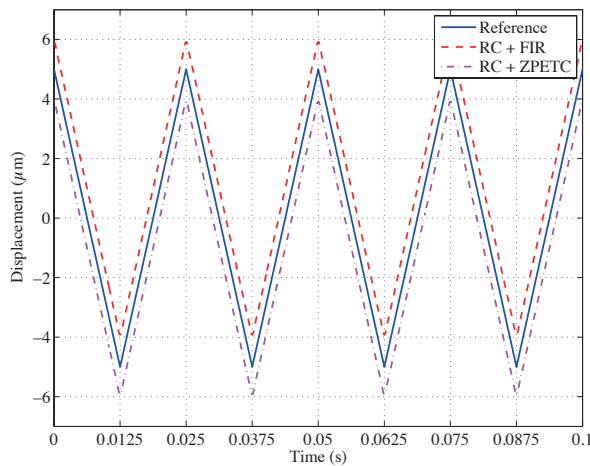


Fig. 11. The measured output displacement. The two measured responses are offset by $\pm 1 \mu\text{m}$ to enhance viewing.

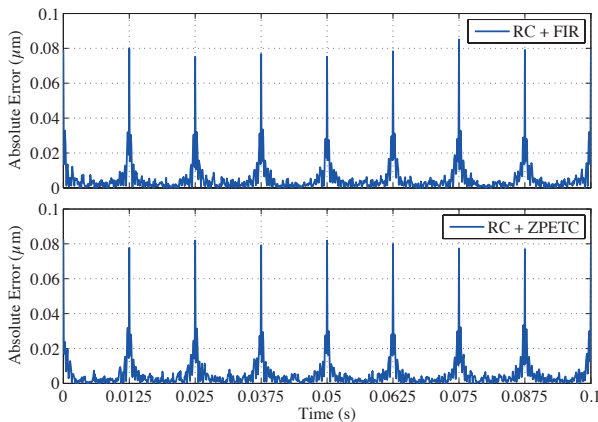


Fig. 12. The output displacement error.

V. CONCLUSION

This paper focused on the design and implementation of a discrete repetitive control scheme when using a model-less finite impulse response (FIR) inverse plant response filter. Methods for obtaining an accurate empirical transfer-function estimate and the synthesis of the FIR inverse from this estimate using the frequency sampling method was presented. The FIR inversion approach was compared to the more common approach of using an infinite impulse response (IIR) filter inverse via the zero-phase error tracking controller (ZPETC) method. The experimental results showed good tracking performance for an experimental nanopositioning system, and further showed that the FIR inverse and the ZPETC inverse had almost identical performance. The main advantages of using the model-less FIR inverse, is that no modeling effort is required, and a more accurate inverse response can in principle be obtained.

ACKNOWLEDGEMENT

This project was supported by the Australian Research Council and the Norwegian University of Science and Technology.

REFERENCES

- [1] S. Hara, Y. Yamamoto, T. Omata, and M. Nakano, "Repetitive Control System: A New Type Servo System for Periodic Exogenous Signals," *IEEE Trans. Autom. Control*, vol. 33, no. 7, pp. 659–668, 1988.
- [2] B. A. Francis and W. M. Wonham, "Internal Model Principle of Control-Theory," *Automatica*, vol. 12, no. 5, pp. 457–465, 1976.
- [3] T. Inoue, M. Nakano, T. Kubo, S. Matsumoto, and H. Baba, "High Accuracy Control of a Proton Synchrotron Magnet Power Supply," in *Proc. 8th IFAC World Congr.*, vol. 20, 1981, pp. 216–221.
- [4] T. Inoue, M. Nakano, and S. Iwai, "High accuracy control of servomechanism for repeated contouring," in *10th Annual Symp. on Incremental Motion Control Systems and Devices*, 1981, pp. 285–292.
- [5] M. Yamada, Z. Riadh, and Y. Funahashi, "Design of Discrete-Time Repetitive Control System for Pole Placement and Application," *IEEE/ASME Trans. Mechatronics*, vol. 4, no. 2, pp. 110–118, 1999.
- [6] C. H. Lee, "Robust Repetitive Control and Application to a CD Player," Ph.D. dissertation, Trinity Hall, Cambridge, 1998.
- [7] J.-H. Moon, M.-N. Lee, and M. J. Chung, "Repetitive Control for the Track-Following Servo System of an Optical Disk Drive," *IEEE Trans. Control Syst. Technol.*, vol. 6, no. 5, pp. 663–670, 1998.
- [8] D. H. Kim and T.-C. Tsao, "Robust Performance Control of Electrohydraulic Actuators for Electronic Cam Motion Generation," *IEEE Trans. Control Syst. Technol.*, vol. 8, no. 2, pp. 220–227, 2000.
- [9] A. J. Fleming, B. J. Kenton, and K. K. Leang, "Bridging the Gap Between Conventional and Video-Speed Scanning Probe Microscopes," *Ultramicroscopy*, vol. 110, no. 9, pp. 1205–1214, 2010.
- [10] Y. Shan and K. K. Leang, "Design and Control for High-Speed Nanopositioning: Serial-Kinematic Nanopositioners and Repetitive Control for Nanofabrication," *IEEE Control Syst. Mag.*, vol. 33, no. 6, pp. 86–105, 2013.
- [11] U. Aridogan, Y. Shan, and K. K. Leang, "Design and Analysis of Discrete-Time Repetitive Control for Scanning Probe Microscopes," *J. Dyn. Syst.-T. ASME*, vol. 131, no. 6, p. 061103 (12 pages), 2009.
- [12] K.-K. Chew, M. Tomizuka, and T.-C. Tsao, "Analysis and Synthesis of Discrete-Time Repetitive Controllers," *J. Dyn. Syst.-T. ASME*, vol. 111, no. 3, pp. 353–358, 1989.
- [13] T. Inoue, "Practical Repetitive Control System Design," in *Proc. 29th IEEE Decis. Contr.*, 1990, pp. 1673–1678.
- [14] Y. Yamamoto, "Learning Control and Related Problems in Infinite-Dimensional Systems," in *Essays on Control: Perspectives in the Theory and Its Applications*. Birkhäuser, 1993, pp. 191–222.
- [15] T. E. Peery and H. Özbay, "On H_∞ optimal repetitive controllers," in *Proc. 32nd IEEE Decis. Contr.*, 1993, pp. 1146–1151.
- [16] J. Li and T.-C. Tsao, "Robust Performance Repetitive Control Systems," *J. Dyn. Syst.-T. ASME*, vol. 123, no. 3, pp. 330–337, 2001.
- [17] A. W. Osburn and M. A. Franchek, "Designing Robust Repetitive Controllers," *J. Dyn. Syst.-T. ASME*, vol. 126, no. 4, pp. 865–872, 2004.
- [18] A. A. Eielsen, J. T. Gravdahl, and K. K. Leang, "Robust Damping PI Repetitive Control for Nanopositioning," in *Proc. 2012 ACC*, Montreal, 2012, pp. 3803–3810.
- [19] —, "Analog Robust Repetitive Control for Nanopositioning Using Bucket Brigade Devices," in *Proc. 19th IFAC World Congr. (to appear)*, Cape Town, 2014.
- [20] B. Panomruttanarug and R. W. Longman, "Designing Optimized FIR Repetitive Controllers from Noisy Frequency Response Data," *Adv. Astronaut. Sci.*, vol. 127, pp. 1723–1742, 2007.
- [21] R. W. Longman, "On the Theory and Design of Linear Repetitive Control Systems," *Eur. J. Control.*, vol. 16, no. 5, pp. 447–496, 2010.
- [22] L. Ljung, *System Identification: Theory for the User*, 2nd ed. Prentice Hall, 1999.
- [23] P. D. Welch, "The Use of Fast Fourier Transform for the Estimation of Power Spectra: A Method Based on Time Averaging Over Short, Modified Periodograms," *IEEE Trans. Audio Electroacoust.*, vol. 15, no. 2, pp. 70–73, 1967.
- [24] L. R. Rabiner, "Techniques for Designing Finite-Duration Impulse-Response Digital Filters," *IEEE Trans. Commun. Technol.*, vol. COM-19, no. 2, pp. 188–195, Apr. 1971.
- [25] M. Tomizuka, "Zero Phase Error Tracking Algorithm for Digital Control," *J. Dyn. Syst.-T. ASME*, vol. 109, no. 1, pp. 65–68, Feb. 1987.
- [26] T. McKelvey, H. Akcay, and L. Ljung, "Subspace Based Multivariable System Identification from Frequency Response Data," *IEEE Trans. Autom. Control*, vol. 41, no. 7, pp. 960–978, 1996.